ELSEVIER

PII: S0144-8617(96)00063-X

Carbohydrate Polymers 30 (1996) 121–127

0144-8617/96/$15.00 + .00

Phase diagrams and molecular structures of sodium-salt-type gellan gum

Y. Izumi,* N. Kikuta, K. Sakai & H. Takezawa

Graduate School of Engineering, Yamagata University, Yonezawa, Yamagata 992, Japan

The phase diagrams of the sodium-salt-type gellan gum solutions with and without salts were established using both mechanical and thermal methods. The transition curves determined by these methods totally disagree. The values for the heat of reaction in kJ/mol of crosslinks, δH, were about 80kJ/mol from the thermal method and 12kJ/mol from the mechanical method. The phase diagrams were divided into 4 regions. The molecular structure in each region was characterized by using small-angle X-ray scattering (SAXS). The results suggest that the mechanical transition indicates the gel–sol transition, while the thermal transition corresponds to a different type of transition like the melting of double helical structures. Two types of gel structures were analyzed using the theory of Oster & Riley (1952). Copyright © 1996 Elsevier Science Ltd

INTRODUCTION

Gellan gum is a microbial polysaccharaide derived from *Pseudomonas elodea*. The polymer contains L-rhamnose, D-glucose, and D-glucuronic acid in the molar ratios 1:2:1 and it has a carboxyl side group (Jansson *et al.*, 1983; O'Neill *et al.*, 1983). Gellan gum is sensitive to the type, valency, and concentration of cations present in salts added to the dispersion before gelation. Physicochemical studies suggest that the junction zones of the gels arise from the association and possibly crystallization of sections of the polymer chain. Acetyl groups inhibit and cations promote such intermolecular association (Carroll *et al.*, 1982; Brownsey *et al.*, 1984). Many studies using potassium-salt-type gellan gum have been performed to study the gel–sol transition for the thermoreversible gel. The results obtained were often controversial because of the difficulty in the preparation of the potassium-salt-type gellan gum employed.

Recently, this situation was altered totally by the advent of the sodium-salt-type gellan gum which dissolves even in cold water. The first study using this sodium-salt-type gellan gum with and without salts was recently performed (Miyoshi *et al.*, 1994a). Many important results on the mechanism of the gel–sol transition in gellan gum solutions were obtained using rheological and DSC techniques. At the same time, however, further detailed studies based on other methods have been required to elucidate the mechanism of gel formation in gellan gum. Following this line of thought, the small-angle X-ray scattering (SAXS) measurements in addition to mechanical and DSC measurements were performed to elucidate the mechanism of the sol–gel transition for these gellan gum solutions with and without salts (Izumi *et al.*, 1994).

*Corresponding author.

EXPERIMENTAL

Materials

The sodium-salt-type gellan gum was supplied by the Kelco Division of Merck & Co. Inc., CA, USA. The contents of the inorganic ions, Na^+, K^+, Ca^{2+} and Mg^{2+} were determined by Kelco using ICP as Na 3.03%, K 0.19%, Ca 0.11% and Mg 0.02%. The number average molecular weight was 4.9×10^4 (Ogawa & Ogino, 1994). NaCl, KCl, $CaCl_2$ and $MgCl_2$ were used as the added salt.

The powdered sample was mixed with water to form a gellan solution in the concentration range from 0.5 to 5wt%. Solutions in the concentration range from 0.5 to 2wt% were prepared for samples containing salts. The concentration of NaCl or KCl in solution ranged from 25 to 180mM or from 5 to 100mM, respectively, and that of $MgCl_2$ or $CaCl_2$ ranged from 2 to 4mM or from 1.5 to 6mM, respectively. The preparation of gellan gum solutions was carried out according to Miyoshi *et al.* (1994a). The gel samples were prepared by quenching into cold water after annealing at 90°C for at least 24h.

Measurements

DSC measurements were carried out using a Seiko DSC 120 equipped with data analysis station for the baseline correction and calculation of the heats of transition. Following preliminary experiments using heating and cooling rates ranging from 0.25 to 3.0°C/min, the DSC measurements were carried out at a constant rate of 0.5°C/min.

The mechanical measurements were made by a visual observation of the onset of the fluidity of the gel on heating. The details are given elsewhere (Tan *et al.*, 1983).

The small-angle X-ray scattering (SAXS) profiles were recorded using synchrotron radiation from the 2.5GeV storage ring at the Photon Factory of the National Laboratory for High Energy Physics, Tsukuba and solution X-ray scattering optics. The details of the optics and instruments are given elsewhere (Ueki *et al.*, 1985).

Scattering data analysis

The scattering data were analyzed in the plot of $hI(h)$ against h, where h equals $(4\pi/\lambda)\sin\Theta$ and $I(h)$ is the scattering intensity at h. This plot, named the Holtzer plot (Holtzer, 1955), is most instructive for the interpretation of rod-like molecules in a dilute solution, as it approaches asymptotically a constant plateau at large h values. As the concentration of the gellan gum solution or the concentration of a salt increases, however, the scattering behavior deviates from the above prediction. The data in this range of concentration were compared with the scattering patterns from aggregates of long cylindrical particles (Oster & Riley, 1952).

RESULTS

Phase diagram without salt

Figure 1 show cooling (a) and heating (b) DSC curves of gellan gum solutions of various concentrations without salt. Only one exothermic peak was observed in cooling DSC curves for all gellan gum concentrations. On the other hand, the splitting of an endothermic peak was observed in the heating DSC curves of higher concentrations than 4.0wt%. The endothermic and exothermic peak temperatures were called melting temperature T_m and setting temperature T_s, respectively (Miyoshi *et al.*, 1994b). The value of T_m almost equals that of T_s in the concentration range less than 3.0wt%. The result suggests that the effect of thermal hysteresis is small in this concentration range.

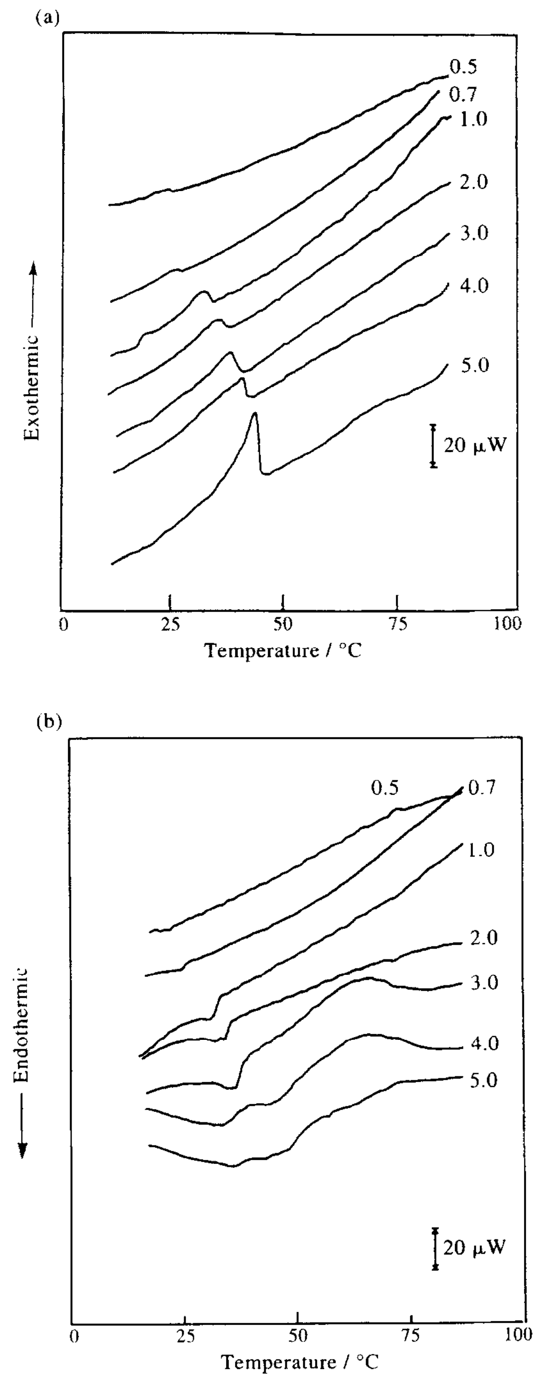

Fig. 1. Cooling (a) and heating (b) DSC curves for gellan gum solutions of various concentrations without salt. Figures beside each curve represent the concentration of gellan gum. Cooling or heating rate: 0.5°C/min.

Figure 2 shows the phase diagram without salt determined by DSC and mechanical methods. The solid and broken lines represent the transition curves determined from the mechanical and thermal measurements, respectively. The value of the heat of reaction in kJ/mol of cross-links, δH, obtained from the broken line was about 80kJ/mol. On the other hand, that obtained from the solid line was about 12kJ/mol. It is clear that the transition curves determined by these methods totally

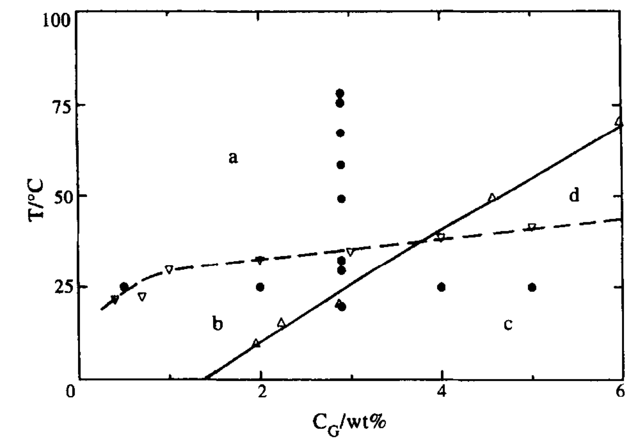

Fig. 2. Phase diagram for gellan gum solutions of various concentrations without salt. The solid and broken lines represent the transition curves determined from the mechanical and thermal measurements, respectively. Filled circles indicate the measuring points by SAXS: (a) sol 1, (b) sol 2, (c) gel 1, (d) gel 2.

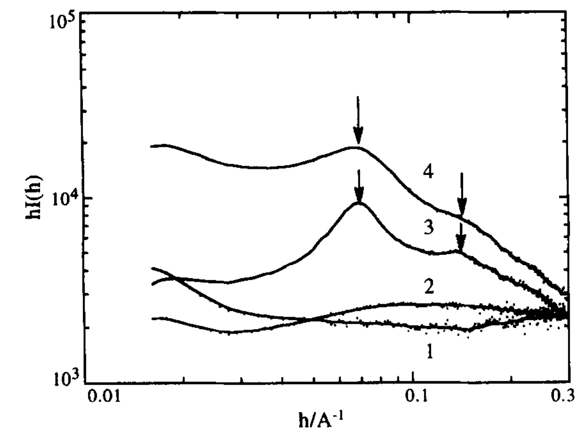

Fig. 3. The Holtzer plots for gellan gum solutions of various concentrations without salt. The arrows indicate two broad peaks around 0.07 and 0.14Å^{-1}. The vertical axis represents the relative scale: 1—0.5wt%, 2—2.0wt%, 3—4.0wt%, 4—5.0wt%.

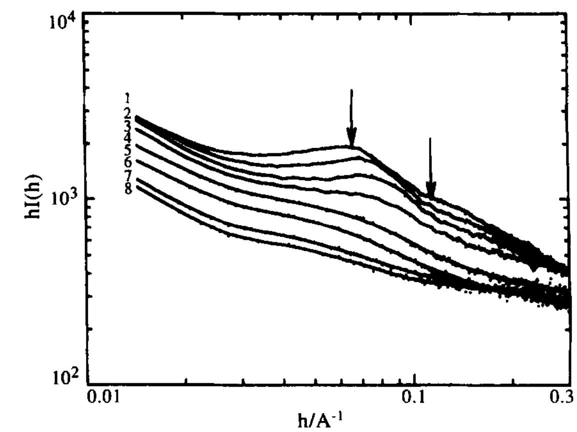

Fig. 4. The temperature variations of the Holtzer plots for 2.9wt% gellan gum solution without salt. The arrows indicate two broad peaks around 0.07 and 0.14Å^{-1}. The vertical axis represents the relative scale: 1—19.8°C, 2—29.5°C, 3—32.2°C, 4—49.2°C, 5—58.5°C, 6—67.3°C, 7—75.5°C, 8—78.1°C.

disagree with each other. Furthermore, the critical gelation concentration, C_{CGC}, is not observed in the thermal transition curve but in the mechanical one. These results suggest that the mechanical transition indicates the gel–sol transition, while the thermal transition corresponds to a different type of transition like the melting of an ordered structure. The phase diagram is then separated into 4 regions by two transition curves. These regions are called sol 1 (a), sol 2 (b), gel 1 (c) and gel 2 (d).

SAXS behaviors without salt

The measuring points are indicated by filled circles in Fig. 2. Figure 3 shows the Holtzer plots for the gellan gum samples without salt as a function of gellan gum concentration at 25°C. The Holtzer plot at 0.5wt% (sol 1) approaches asymptotically a constant plateau at large h values. This asymptote is indicative of the rigid-rod behavior of the long section of the chain (Holtzer, 1955). The experimental evidence for the rigid-like behavior for the gellan gum molecule has been given by light scattering measurement in dilute solution (Dentini *et al.*, 1988). As the concentration increases, the Holtzer plots are characterized by the appearance of a broad peak around $h = 0.1$ Å^{-1} at 2wt% (sol 2) and two broad peaks around 0.07 and 0.14Å^{-1} at 4 and 5wt% (gel 1), respectively. Noting that the thermal and mechanical transitions occur at 0.7 and 3wt%, respectively, three regions (sol 1, sol 2 and gel 1) in the phase diagram were confirmed by the SAXS profiles.

Figure 4 shows the temperature variations of the Holtzer plots at 2.9wt%. As the temperature is elevated, the two broad peaks characteristic of gel 1 vanish, a broad peak appears around $h = 0.08$ A^{-1} at about 32°C and finally disappears at an elevated temperature. Noting that the mechanical and thermal transitions occur at 25 and 35°C, respectively, each region in the phase diagram was not confirmed rigorously by the SAXS profile. This may be caused by a technical problem (e.g. the position of the temperature sensor).

Phase diagrams with monovalent salt

Figure 5 shows cooling DSC curves of 0.5wt% gellan gum solutions with NaCl (a) and KCl (b) of various concentrations, respectively. A single exothermic peak was observed in these cooling DSC curves. Here, the concentration of gellan gum was fixed at 0.5wt%, because the solution behavior without salt was typical of a dilute solution.

Figure 6 shows the phase diagrams of 0.5wt% gellan gum solutions with NaCl (a) and KCl (b), respectively. The solid and broken lines represent the transition curves determined from the mechanical and DSC

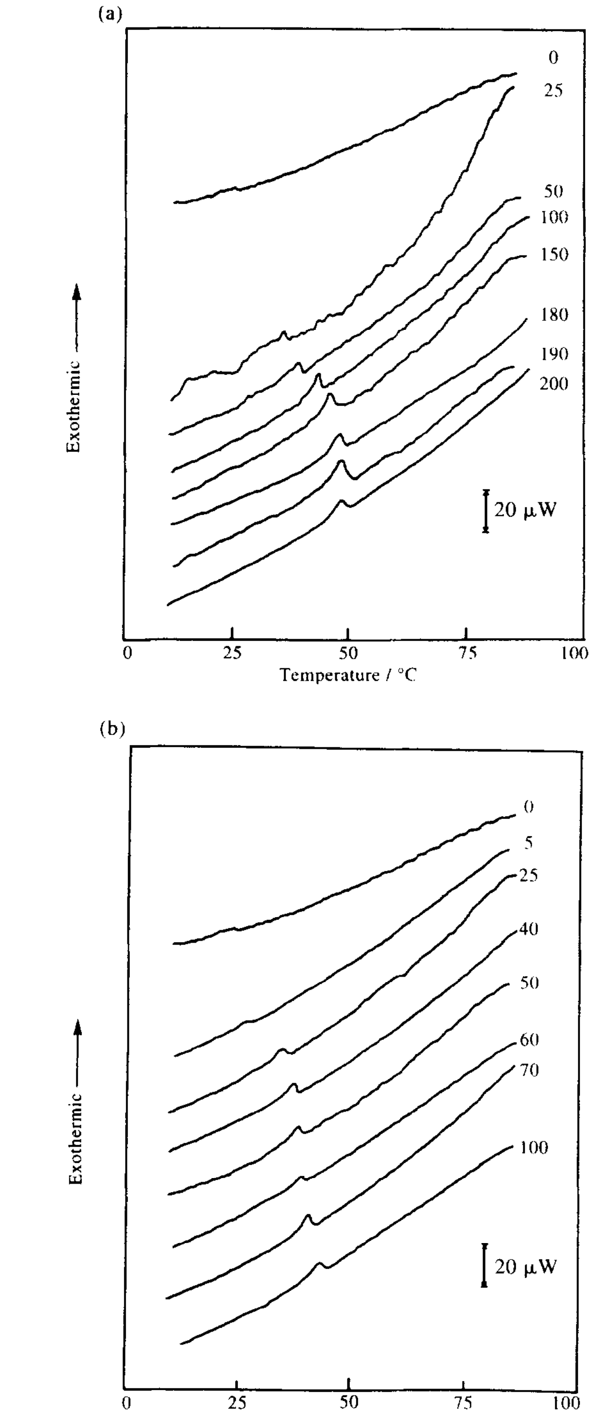

Fig. 5. Cooling DSC curves for 0.5wt% gellan gum solutions containing NaCl (a) and KCl (b) of various concentrations. Figures beside each curve represent the concentration of each salt. Cooling rate: 0.5°C/min.

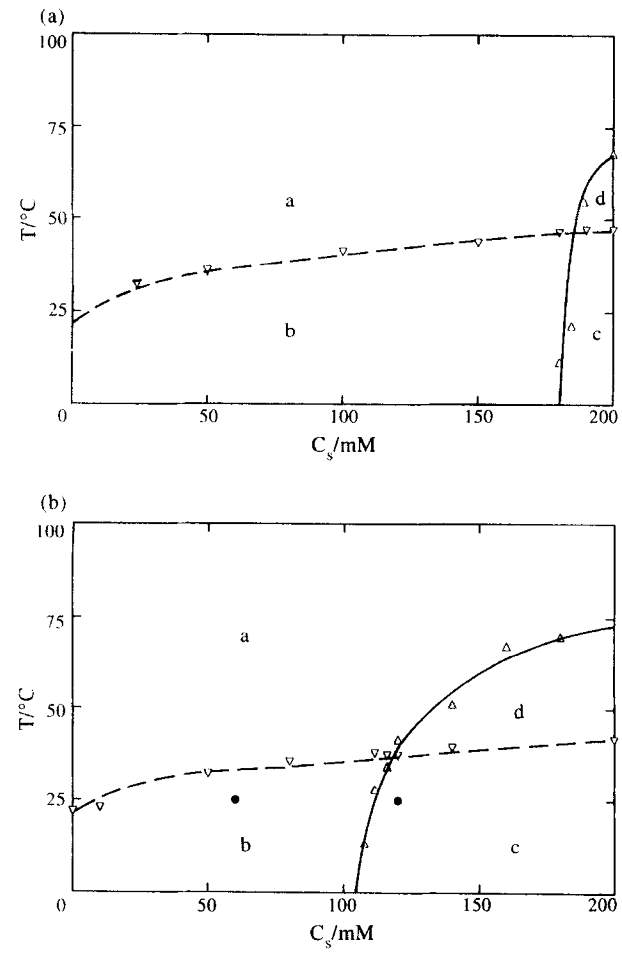

Fig. 6. Phase diagram for 0.5wt% gellan gum solutions containing NaCl (a) and KCl (b) of various concentrations. The significance of other symbols is the same as in Fig. 2.

measurements, respectively. Each phase diagram is distinguished into 4 regions by the two transition curves: sol 1, sol 2, gel 1 and gel 2. In each phase diagram, the transition curves determined by these methods totally disagree. Comparing Fig. 6(a) with 6(b), the thermal transition curve for KCl almost agrees with that for NaCl, while the mechanical transition curve for KCl is totally different from that for NaCl. A C_{CGC} is not observed in the thermal transition curve but in the mechanical one. These results suggest the mechanical transition corresponds to the gel–sol transition, while the thermal transition corresponds to a different type of transition like the melting of a local ordered structure. The value of C_{CGC} for the sample containing KCl is about 1/3 of that containing NaCl. The result indicates that potassium ions are more effective in enhancing the gelling ability (Moritaka *et al.*, 1992; Miyoshi *et al.*, 1994b).

SAXS behaviors with monovalent salt

The measuring points are indicated by filled circles in Fig. 6. Figure 7 shows the Holtzer plots for the gellan gum samples at 30 and 60mM KCl. The Holtzer plot for 30mM KCl (sol 2) is slightly different from that of the same gellan gum concentration without salt shown in Fig. 3. On the other hand, the Holtzer plot for 60mM KCl (gel 1) is characterized by an increase of small angle scattering in the range of h smaller than $0.2Å^{-1}$. The increase is accompanied by the formation of a gel

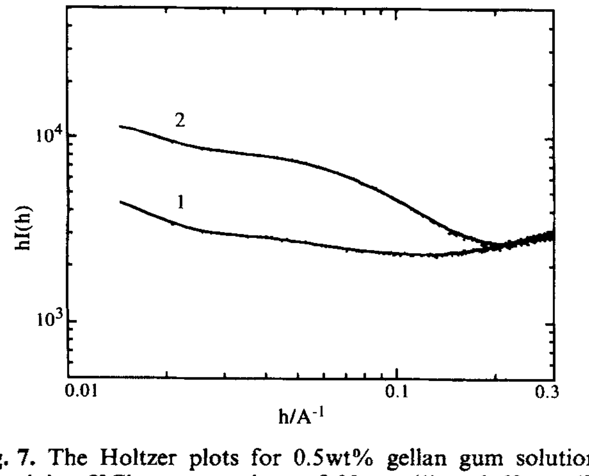

Fig. 7. The Holtzer plots for 0.5wt% gellan gum solutions containing KCl concentrations of 30mM (1) and 60mM (2). The vertical axis represents the relative scale.

structure. Noting that the mechanical transition occurs at 55mM, two regions (sol 2 and gel 1) in the phase diagram were confirmed by the SAXS profiles. It is noted that the gel structure in this case is very different from that without salt.

Phase diagrams with divalent salt

Figures 8 and 9 show the phase diagrams of gellan gum solutions with $MgCl_2$ and $CaCl_2$, respectively. The solid lines represent the transition curves determined by the mechanical measurements. The broken lines represent the thermal transition curves cited from the data of Miyoshi *et al.* (1994b). Each phase diagram was divided into 4 regions by the two transition curves: sol 1, sol 2, gel 1 and gel 2. In each phase diagram, the two transi-

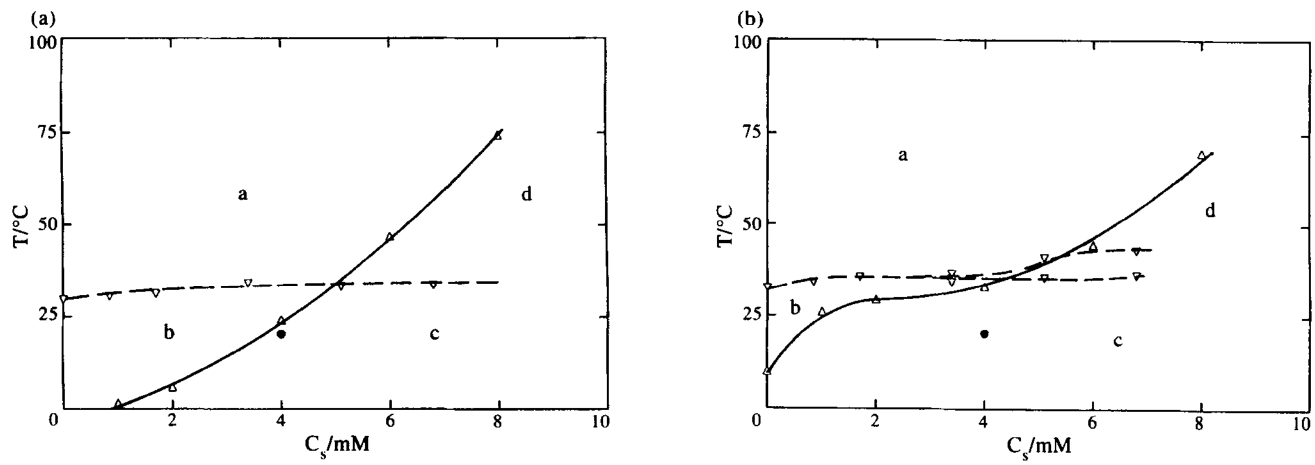

Fig. 8. Phase diagram for 1.0 (a) and 2.0wt% (b) gellan gum solutions containing $MgCl_2$ of various concentrations. The broken lines represent the transition curves cited from the data of Miyoshi et al. (1994b). The significance of symbols is the same as in Fig. 2.

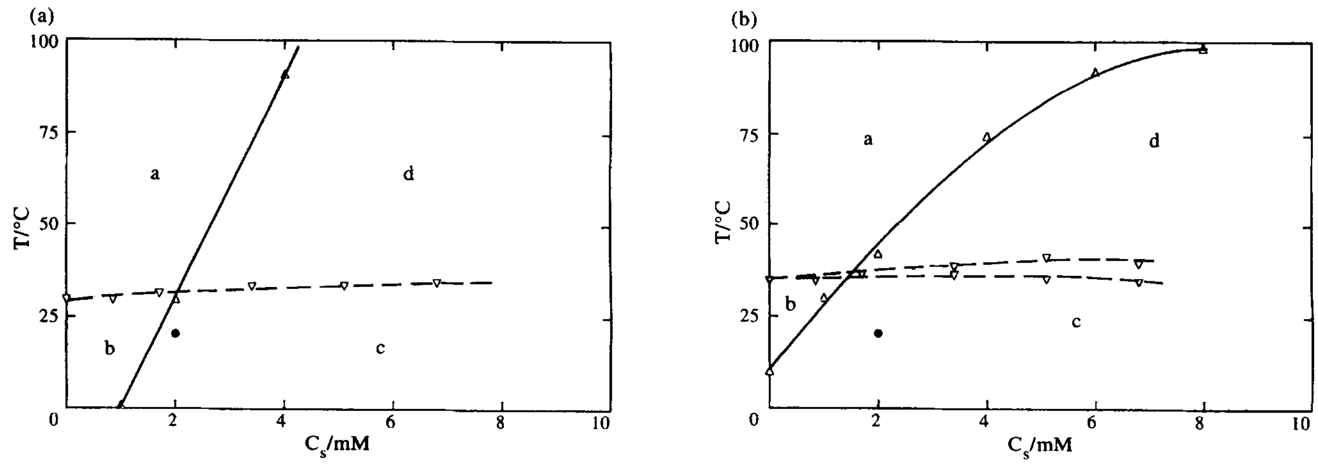

Fig. 9. Phase diagram for 1.0 (a) and 2.0wt% (b) gellan gum solutions containing $CaCl_2$ of various concentrations. The broken lines represent the transition curves cited from the data of Miyoshi et al. (1994b). The significance of the symbols is the same as in Fig. 2.

tion curves totally disagree. From Figs 8 and 9, the thermal transition is not sensitive to the type of salt, while the mechanical transition is very sensitive. A C_{CGC} is not observed in the thermal transition curve. On the other hand, a C_{CGC} is observed in the mechanical transition curve for the 1 wt% gellan gum solution. These results support that the mechanical transition corresponds to the gel–sol transition, while the thermal transition corresponds to a different type of transition like the melting of a local ordered structure. The value of C_{CGC} for the sample containing $MgCl_2$ almost equals that containing $CaCl_2$, but the increase in the temperature of the mechanical transition with electrolyte concentration for the former is less pronounced than for the latter. The result indicates that the calcium ion is more effective in enhancing the gelling ability (Miyoshi *et al.*, 1994b).

SAXS behaviors with divalent salt

The measuring points are indicated by filled circles in Figs 8 and 9. Figure 10 show the Holtzer plots for the gellan gum samples containing $MgCl_2$ (a) and $CaCl_2$ (b), respectively. The SAXS behavior in gel 1 is affected significantly by the concentration of gellan gum, although it is not affected very much by the type of divalent salts. The Holtzer plots at 2wt% are characterized by the appearance of two or three peaks around 0.05, 0.1 and 0.2Å^{-1}.

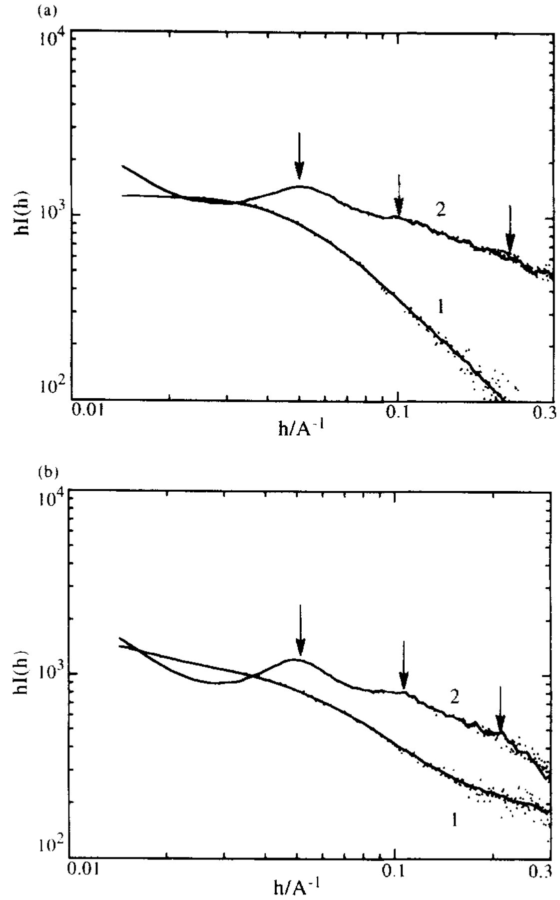

Fig. 10. The Holtzer plots for 1.0 (1) and 2.0wt% (2) gellan gum solutions containing $MgCl_2$ (a) or $CaCl_2$ (b) of various concentrations. The arrows indicate three broad peaks around 0.05, 0.1 and 0.2Å^{-1}. The vertical axis represents the relative scale.

DISCUSSION

It is worth modelling the structural changes which are accompanied by the increase of gellan gum concentration. The gellan gum molecule in a dilute solution is approximated by a long cylindrical particle of radius R of linear mass M_L from the scattering behavior at 0.5wt%. The expression for the scattering intensity by parallel cylindrical particles of infinite length (Oster & Riley, 1952) could be applicable to SAXS from the gel 1.

Figure 11 shows the calculated curves with $R=5$Å, $\delta=4$Å and $c=0$ (No. 1), $R=70$Å, $\delta=10$Å and $c=0$ (No. 2) and $R=70$Å, $\delta=10$Å and $c=0.8$ (No. 3), where δ represents a parameter for the size distribution for R and $R(1-c)$ is the thickness of the cylindrical shell. The calculated curve for No. 1 corresponds to the SAXS profile at 0.5wt% without salt. The calculated curve of Nos 2 and 3 corresponds to the SAXS profiles of 4 and 5wt% gellan gum gels without salt and those of 2wt% gels with divalent salt. The result suggests the existence of aggregates of cylinders with $R=70$Å in this type of gel.

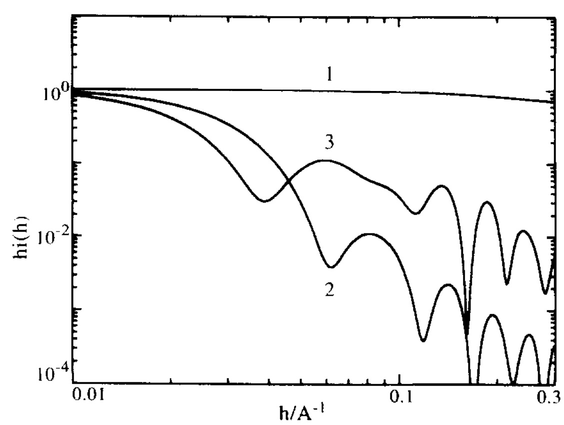

Fig. 11. The calculated scattering curves with $R=5$Å, $\delta=4$Å and $c=0$ (No. 1), $R=70$Å, $\delta=10$Å and $c=0$ (No. 2) and $R=70$Å, $\delta=10$Å and $c=0.8$ (No. 3), where δ represents a parameter for the size distribution for the radius R and $R(1-c)$ is the thickness of the cylindrical shell.

Figure 12 shows the calculated curves with $R=5$Å, $\delta=0$, $c=0$ and $\gamma=0$ (No. 1), $\gamma=2$ (No. 2), $\gamma=2.25$ (No. 3), where γ is the swelling parameter defined by $d/2R$, d being the interparticle distance separating the centres of nearest neighbours. The calculated curve for No. 2 corresponds to the SAXS profile of 0.5wt% gellan gum gel at 60mM KCl. The result

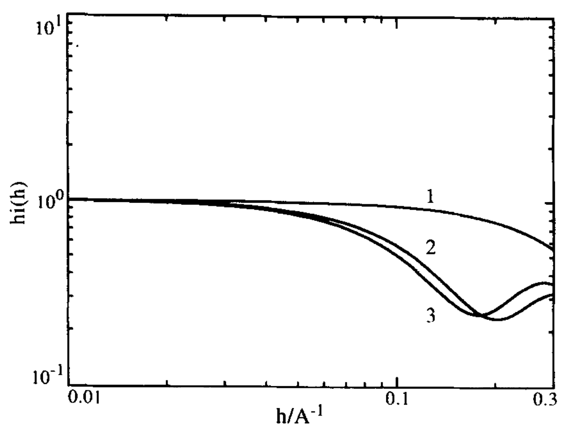

Fig. 12. The calculated curves with $R=5$Å, $\delta=0$, $c=0$ and $\gamma=0$ (No. 1), $\gamma=2$ (No. 2), $\gamma=2.25$ (No. 3), where γ is the swelling parameter defined by $d/2R$, d being the interparticle distance separating the centres of nearest neighbours.

suggests the existence of aggregates of two parallel cylinders in this type of gel.

CONCLUSIONS

The transition curves determined by thermal and mechanical methods totally disagree with each other. The values of the heat reaction in kJ/mol of crosslinks, δH, were about 80kJ/mol from the thermal method and 12kJ/mol from mechanical method, respectively. The phase diagrams were separated into 4 regions. The results suggest that the mechanical transition corresponds to the gel–sol transition, while the thermal transition corresponds to a different type of transition like the melting of a local ordered structure. The gel structures accompanied by the gel–sol transition could be partly described by a model consisting of parallel cylindrical particles.

ACKNOWLEDGEMENTS

The authors thank Dr G. Sanderson of Kelco Division of Merck & Co. Inc., CA, USA, for the gift of the sodium form of gellan gum. The authors also thank Prof. K. Nishinari of Osaka City University, Osaka, Japan, for the distribution of the sample as well as making available manuscripts prior to the publication. This work was supported by the Photon Factory Advisory Committee Proposal No. 93G-226, Tsukuba, Japan.

REFERENCES

Brownsey, G. J., Chilvers, G. R., I'Anson, K. J. & Morris, V. J. (1984). *Int. J. Biol. Macromolecules*, **6**, 211–214.
Carroll, V., Miles, M. J. & Morris, V. J. (1982). *Int. J. Biol. Macromolecules*, **4**, 432–433.
Dentini, M., Coviello, T., Burchard, W. & Crescenzi, V. (1988). *Macromolecules*, **21**, 3312–3320.
Izumi, Y., Iwano, S., Kikuta, N. & Sakai, K. (1994). *Rep. Progr. Polym. Phys. Jpn*, **37**, 645–648.
Jansson, P., Lindberg, B. & Sandford, P. A. (1983). *Carbohydr. Res.*, **124**, 135–139.
Miyoshi, E., Takaya, T. & Nishinari, K. (1994a). *Rep. Progr. Polym. Phys. Jpn*, **37**, 751–754.
Miyoshi, E., Takaya, T. & Nishinari, K. (1994a). *Food Hydrocolloids*, **8**, 505–527, 529–542.
Moritaka, H., Nishinari, K., Nakahama, N. & Fukuba, H. (1992). *Biosci. Biotech. Biochem.*, **56**, 595–599.
Ogawa, E. & Ogino, K. (1994). *Rep. Progr. Polym. Phys. Jpn*, **37**, 695–698.
O'Neill, M. A., Selvendran, R. R. & Morris, V. J. (1983). *Carbohydr. Res.*, **124**, 123–133.
Oster, G. & Riley, D. P. (1952). *Acta Crystallogr.*, **5**, 272–276.
Tan, H. M., Moet, A., Hiltner, A. & Baer, E. (1983). *Macromolecules*, **16**, 28–34.
Ueki, T., Hiragi, Y., Kataoka, M., Inoko, Y., Amemiya, Y., Izumi, Y., Tagawa, H. & Muroga, Y. (1985). *Biophys. Chem.*, **23**, 115–124.